Epilepsy Research 127 (2016) 141–151

Contents lists available at www.sciencedirect.com

Epilepsy Research

journal homepage: www.elsevier.com/locate/epilepsyres

# Alterations in *BRAF* gene, and enhanced mTOR and MAPK signaling in dysembryoplastic neuroepithelial tumors (DNTs)

Aanchal Kakkar[a,1], Atreye Majumdar[a,1], Anupam Kumar[a], Manjari Tripathi[b], Pankaj Pathak[a], Mehar C. Sharma[a], Vaishali Suri[a], Vivek Tandon[c], Sarat P. Chandra[c], Chitra Sarkar[a,*]

[a] *Department of Pathology, All India Institute of Medical Sciences, New Delhi, India*
[b] *Department of Neurology, All India Institute of Medical Sciences, New Delhi, India*
[c] *Department of Neurosurgery, All India Institute of Medical Sciences, New Delhi, India*

ARTICLE INFO

*Article history:*
Received 24 February 2016
Received in revised form 11 August 2016
Accepted 23 August 2016
Available online 28 August 2016

*Keywords:*
Dysembryoplastic neuroepithelial tumor
Epilepsy
*BRAF*
mTOR
MAPK

ABSTRACT

*Objective:* Recently, *BRAF* V600E mutation, and activation of mTOR and MAPK pathways have been identified in various glial/glioneuronal tumors. Dysembryoplastic neuroepithelial tumors (DNTs) are epilepsy-associated glioneuronal neoplasms which have not been analyzed extensively in this respect.
*Methods:* Sequencing for *BRAF* V600E mutation, analysis of *BRAF* copy number by qRT-PCR, and immunohistochemistry for mTOR (p-S6, p-4EBP1) and MAPK (p-MAPK) pathways were performed.
*Results:* Sixty-four DNTs were identified, accounting for 15.1% of patients with drug-refractory epilepsy (mean age: 15.5 years). Duration of seizures ranged from 1 to 22 years. *BRAF* V600E mutation was identified in 3.7% of DNTs, while *BRAF* copy number gain was observed in 33.3%. mTOR-pathway activation indicated by p-S6 or p-4EBP1 immunopositivity was seen in 89.7% cases. Interestingly, p-S6 positivity was also seen in adjacent dysplastic cortex. p-MAPK immunopositivity was seen in 50% cases. MAPK and mTOR pathway activation was independent of *BRAF* alterations. All patients that underwent incomplete resection had Engel grade II–III outcomes ($p < 0.001$).
*Conclusion:* *BRAF* alterations are frequent in DNTs, particularly *BRAF* copy number gain which is being reported for the first time in these tumors. Evidence of activation of mTOR and MAPK pathways suggests a role for altered signalling in DNT pathogenesis, and will pave the way for development of targeted therapies, particularly relevant for patients having persistent seizures after incomplete resection.


## 1. Introduction

DNT is a benign glioneuronal neoplasm, corresponding to WHO grade I, that is seen predominantly in children and young adults, and characteristically occurs as a multinodular tumor in the temporal cortex (Lee et al., 2015; Sharma et al., 2009). DNTs account for 10–20% of histologic diagnoses in adult epilepsy series, with a frequency of 9% from a large series of Indian patients (Sarkar et al., 2006). Clinically, most patients present with drug-refractory complex partial seizures with or without secondary generalization (Daumas-Duport et al., 1988; Lee et al., 2009), and with onset of seizures in late childhood (median age: 7–13 years) (Lee et al., 2009; Sharma et al., 2009). Morphologically, DNTs show considerable heterogeneity, including simple, complex, and non-specific/diffuse forms (Daumas-Duport et al., 1988; Sharma et al., 2009). The adjoining cortex often shows features of focal cortical dysplasia (FCD), and is postulated to play a role in the epileptogenicity of these tumors (Daumas-Duport et al., 1988; Lee et al., 2009; Sakuta et al., 2005; Sharma et al., 2009; Takahashi et al., 2005). DNTs are considered to be surgically curable, with the rate of seizure –free outcome after excision ranging from approximately 70–100% (Chan et al., 2006; Kirkpatrick et al., 1993; Lee et al., 2000; Lee et al., 2009; Sandberg et al., 2005; Sharma et al., 2009). However, in some instances, surgical failure might occur due to incomplete tumor removal, or presence of dysplastic cortex adjacent to the tumor which is not resected (Lee et al., 2009). In addition, long duration of epilepsy and older age at the time of surgery have been reported to decrease the probability of achieving a good seizure-free outcome (Lee et al., 2009). The utility of electrocorticography

* Corresponding author at: Department of Pathology, All India Institute of Medical Sciences, New Delhi-110029, India.
*E-mail address:* sarkar.chitra@gmail.com (C. Sarkar).
[1] Aanchal Kakkar and Atreye Majumdar have contributed equally and are to be considered as co- first authors.

http://dx.doi.org/10.1016/j.eplepsyres.2016.08.028
0920-1211/

(ECoG) or intraoperative electroencephalography (EEG) in resection of DNTs has been debated in literature. While some studies have not shown improvement in outcome with ECoG-guidance (Lee et al., 2000), others have demonstrated significant benefit (Sandberg et al., 2005).

Alterations in *BRAF*, an oncogene, have been described in various human cancers, including malignant melanoma, papillary carcinoma of thyroid, and hairy cell leukemia (Berghoff and Preusser, 2014). The most common alteration seen is the V600E mutation in exon 15, wherein a valine (V) to a glutamic acid (E) amino acid substitution occurs at position 600. This mutation occurs within the activation segment of the kinase domain leading to constitutive activation of *BRAF* and the downstream MAP kinase (MAPK) pathway. Other alterations in the *BRAF* gene include the *BRAF*-KIAA1549 fusion seen in pilocytic astrocytomas (Collins et al., 2015), and copy number variations seen in various cancers, such as lung and prostate adenocarcinoma (Ren et al., 2012; Sasaki et al., 2015). Recent studies have demonstrated *BRAF* V600E mutation in various glial and glioneuronal tumors, especially gangliogliomas (GGs) and pleomorphic xanthoastrocytomas (PXAs) with a wide ranging frequency (Dougherty et al., 2010; Horbinski et al., 2012; Schindler et al., 2011). Copy number aberrations identified in DNTs include gain of chromosome 7q, on which *BRAF* is located; however, gain of *BRAF* locus has not been reported (Prabowo et al., 2015). While activation of the MAPK pathway has been identified in pilocytic astrocytomas, this pathway has not been analysed in DNTs (Jones et al., 2012). The importance of identifying *BRAF* alterations and activation of its downstream pathways lies in the fact that the protein product of the mutant gene is sensitive to *BRAF* inhibitors such as vemurafenib, while MEK inhibitors block MAPK signalling, as evidenced by clinical trials in malignant melanoma (Chapman et al., 2011; Flaherty et al., 2012).

The mTOR signalling pathway has recently been shown to be activated in FCD as well as in pediatric low grade gliomas, including pilocytic astrocytomas and PXAs, the latter of which are known to present with intractable seizures (Hütt-Cabezas et al., 2013). As p-S6 immunopositivity was frequently noted in PXAs, which are typically associated with *BRAF* mutation, it has been suggested that *BRAF* mutations may alter mTOR signalling (Hütt-Cabezas et al., 2013). Further, the association of *BRAF* mutation with enhanced mTOR pathway signalling has been described in neoplasms outside of the CNS, such as papillary thyroid carcinoma (Faustino et al., 2012). Thus, identification of *BRAF* alterations and of specific mTOR pathway effectors that are activated in DNTs would pave the way for discovery of newer selective drugs to treat intractable epilepsy (Galanopoulou et al., 2012).

Presently, there are very few centres in India that perform epilepsy surgery, and there is no large study on DNTs with adequate follow-up. We therefore conducted this study with the aims of analyzing DNTs for i) clinical, histopathological and immunohistochemical characteristics; ii) alterations in the *BRAF* gene; and iii) presence of mTOR and MAPK pathway activation, and to correlate the latter two with clinicopathological features, especially seizure outcome after surgery.

## 2. Materials and methods

All cases of DNT diagnosed in the Neuropathology laboratory at our Institute over a 14-year (2002–2015) period were identified. Clinical data was obtained, including demographic details, tumor location, symptoms at presentation along with duration, EEG findings, surgical procedure undergone, extent of resection, and follow-up after surgery. Seizure control outcome following surgery was classified using the Engel system (Engel, 1993). Approval was obtained from the Institutional Ethics Committee for experiments conducted on human patient samples. Hematoxylin and eosin (HE) stained slides were retrieved, and histopathological features were reviewed, along with immunohistochemistry that had been performed originally for confirmation of diagnosis, including GFAP, NeuN, CD34, and synaptophysin. All cases were classified according to the WHO 2007 classification; ILAE classification was followed for classification of FCD (Blümcke et al., 2011).

### 2.1. Immunohistochemistry for mTOR signalling pathway activation

Immunohistochemistry was performed on cases with adequate tissue in blocks using the following antibodies from Cell Signaling Technology, Beverly, MA, USA: p-S6 (dil 1:400) and p-4EBP1 (dil 1:1400) for mTOR pathway, and p-44/42 MAPK (Erk1/2) (dil 1:50) for MAPK pathway. The procedure followed was as reported previously (Kakkar et al., 2015). The staining was scored as follows based on the percentage of tumor cells showing moderate to marked immunopositivity: 0: negative/rare positive cells, 1+: 1%–10% positive cells, 2+: 10%–50% positive cells, and 3+: ≥50% positive cells; 2+ and 3+ staining was considered as positive (Hütt-Cabezas et al., 2013).

### 2.2. Sequencing for BRAF V600E mutation

DNA was extracted from fresh frozen tissue where available (11 cases), and FFPE tissue (16 cases) using QIAmp DNA mini kit (M/s Qiagen, S.A., Courtaboeuf, France) and Ambion RecoverAll Total Nucleic Acid Isolation kit (M/s Life Technologies, Carlsbad, CA, USA), respectively, according to the manufacturer's instructions. The remaining 37 cases either did not have sufficient tissue for DNA extraction in the paraffin blocks after performing immunohistochemistry, or the DNA extracted was of inferior quality. Thus, genetic analysis could not be performed on them. DNA concentration was quantified by Picodrop Microliter UV/Vis Spectrophotometer and its integrity was checked on 2% agarose gel. Similarly, blood DNA from 8 normal controls was extracted using the QIAmp DNA mini kit (M/s Qiagen, S.A., Courtaboeuf, France). The samples were stored at −20° C until further use. Approximately 50 ng of DNA was used to amplify the *BRAF* (codon 600) gene by polymerase chain reaction (PCR). Primer pairs used were 5′- TCATAATGCTTGCTCTGATAGGA-3′ (forward) and 5′-GGCCAAAAATTTAATCAGTGG A-3′ (reverse). The cycling conditions for a 25 μl PCR were initial denaturing at 95° C for 5 mins, followed by 35 cycles of denaturation at 95° C for 30 s, annealing at 60° C for 30 s and extension at 70° C for 30 s. A final extension was given at 72° C for 10 min. The PCR purified product was further subjected to bidirectional sequencing using the BigDye terminator v3.1 cycle sequencing kit (Applied Biosystems, Foster City, CA, USA) with the primers used to perform the PCR. Purified sequencing reaction product was sequenced using ABI 3730 DNA analyser (Applied Biosystems, Foster City, CA, USA). The generated sequencing data was analysed with DNAstar software (DNAstar Inc, Madison, WI, USA).

### 2.3. Quantitative real-time PCR for BRAF copy number gain

Quantitative real-time PCR using Stratagene Mx3000P (Agilent, USA) was performed on DNA extracted from tumor (n = 27) and control (n = 6) samples, and 20 ng of DNA was used in a 10 μl reaction to detect *BRAF* gene copy number gain. GAPDH and CF genes were used as internal controls for all the samples and SYBR green dye was the detection reagent. Primer pairs used were 5′-TTCATGAAGACCTCACAGTAAAAA-3′ (forward) and 5′-CCACAAAATGGATCCAGACA-3′ (reverse). The relative copy number gain of the target in the sample was determined by using the

comparative Ct (threshold cycle) method, as described previously (Biernat et al., 2004; Kumar et al., 2015; Nigro et al., 2001) Tumor samples were considered to be positive for *BRAF* gain when PCR reactions using both the reference genes (GAPDH and CF) showed more than 4-fold copy-number gain.

## 3. Results

Sixty-four cases of DNT were diagnosed over the 14-year period, which accounted for 15.1% of refractory epilepsy-associated lesions on histopathology. The mean age of patients included was 15.5 years, with range of 2–37 years. A male preponderance was noted, with 48 males and 16 females. Majority (46/64; 71.9%) of patients were in the pediatric age group (≤18 years). Clinical details were available for all 64 patients, all of whom presented with history of seizures that were refractory to medical treatment. The age of onset of seizures ranged from 1 to 24 years of age (mean = 8 years), and was most frequently in the first decade of life (47/64; 73.4%). Duration of seizures ranged from 1 to 22 years (mean = 7.5 years). At the time of surgery, majority of patients were in the second decade of life (33 patients; 51.6%), while 18 patients (28.1%) were in the first decade of life, and 13 patients (20.3%) were older than 20 years. A little more than half the tumors were located in the temporal cortex (36 cases; 56.2%); the second most common location was the frontal cortex (14 cases; 21.9%); rare locations included parietal (9 cases; 14.1%) and occipital (4 cases; 6.2%) cortex, and posterior fossa (1 case; 1.6%). All patients underwent ECOG-guided resection. Two patients (Cases 51 and 60) had been operated elsewhere initially and underwent resection of the residual tumors. Sixty tumors (93.8%) were completely resected, while the remainder were incompletely resected. Clinical details of patients included are shown in Table 1.

### 3.1. Histopathology

All cases were characterized by presence of cortical nodules composed of the specific glioneuronal element, i.e. perpendicular arrays of oligodendroglial- like cells in a mucoid background, with interspersed floating neurons that were immunopositive for NeuN (Fig. 1A–D). Complex DNTs with an additional component of glial nodules accounted for 47 cases (73.4%), while the remaining were simple DNTs. Calcification was seen in 25 cases (39.1%), eosinophilic granular bodies in 14 cases (21.9%), hyalinised vessels in 8 cases (12.5%), and garlanding vessels in 12 cases (18.8%). Nuclear atypia and leptomeningeal spread were rarely encountered, being present in two (3.1%) and four (6.2%) cases, respectively. The adjoining cortex showed loss of laminar architecture highlighted on NeuN staining. Dysplastic neurons showed CD34 immunopositivity in a bush-like pattern (Fig. 1E–H). These features of FCD type IIIb were seen in 49 cases (76.6%). Hippocampus included in the surgical specimens showed features of mesial temporal sclerosis (MTS) in three cases (4.7%).

### 3.2. Immunohistochemistry for mTOR and MAPK pathway activation (Fig. 3)

Cytoplasmic immunopositivity for pS6 was seen in 26/29 (89.7%) cases examined. Of these, 10 showed 2+ staining (Fig. 2A) while 16 showed 3+ staining (Fig. 2B). Immunopositivity was restricted to the neuronal cells in most cases (Fig. 2C); four cases showed immunoreactivity in the astrocytic component as well. On the other hand, immunoreactivity for p-4EBP1 was seen in 6/24 cases (25%), predominantly in neuronal cells (Fig. 3A,B). All positive cases had a score of 2+; no 3+ score cases were seen. All cases positive for p-4EBP1 were also positive for p-S6 (3+ positivity), while all cases negative for p-S6 were also negative for p-4EBP1. Thus, mTOR pathway activation, indicated by positivity for either marker, was seen in 89.7% of cases. All cases with FCD showed p-S6 immunopositivity in the tumor. Interestingly, in 7 cases, neurons in the adjacent dysplastic cortex also showed immunoreactivity for p-S6 (Fig. 2D); however, this was not seen with p-4EBP1. p-MAPK immunopositivity was seen in 10/20 (50%) cases examined (Fig. 3C,D). Of these, majority showed 3+ positivity (8 cases). No significant association was noted between immunoreactivity and patient age, sex, tumor location and seizure outcome.

### 3.3. BRAF V600E mutation and copy number gain

On evaluation, *BRAF* V600E mutation (Fig. 4) was detected in only 1 out of 27 cases (3.7%), while *BRAF* copy number gain was observed in 9 out of 27 cases (33.3%). Thus, 10 out of 27 (37%) cases analyzed showed *BRAF* alterations. None of the cases showing *BRAF* copy number gain demonstrated *BRAF* V600E mutation. On correlation with immunohistochemical expression of mTOR and MAPK pathway markers, evidence of activation of MAPK and mTOR pathways was seen in cases with as well as without *BRAF* alterations. No significant association was noted between *BRAF* alterations and clinicopathological features. Results of immunohistochemical and molecular analyses are shown in Table 1.

### 3.4. Follow-up

On follow-up ranging from 1 to 10 years in duration, 55/64 (85.9%) patients were seizure-free with Engel grade I outcome; seven patients (10.9%) had Engel grade II and two (3.2%) had Engel grade III outcomes at last follow-up (Table 1). On correlation with extent of resection, all patients with Engel grade I outcome (55 cases) had been completely resected, while all tumors that had been incompletely resected (4 cases) had Engel grade II/III outcome, and the association of extent of resection with outcome was statistically significant ($p < 0.001$). Both patients with residual tumors had Engel grade III outcome after first surgery, which improved to Engel grade I following excision of the residual tumors. No correlation was noted between outcome and other clinicopathological parameters, including age at seizure onset, duration of seizures, sex, tumor location, *BRAF* alterations and immunoexpression of p-S6/p-4EBP1/p-MAPK.

## 4. Discussion

*BRAF*, or β-Rapidly accelerated fibrosarcoma gene, is an oncogene located on chromosome 7q34. It encodes for a member of the serine/threonine kinase family, which acts as an immediate downstream effector of RAS in the MAPK signalling cascade. Recent studies have identified *BRAF* mutations in various epilepsy-associated tumors, including PXA, GG and also in DNTs. While few studies on DNTs did not identify *BRAF* mutation in any of the cases analyzed (Dougherty et al., 2010; Gessi et al., 2016; Horbinski et al., 2012; Schindler et al., 2011; Rivera et al., 2016; Zhang et al., 2013), other studies on larger number of cases have identified *BRAF* V600E mutation in 30–50% of DNT cases examined (Chappe et al., 2013; Gierke et al., 2016; Lee et al., 2015; Prabowo et al., 2014). While most studies have performed sequencing for detection of the mutation, Prabowo et al. (2014) performed IHC with a *BRAF* V600E mutation-specific antibody as well, and reported immunoreactivity in 23/77 (29.8%) of DNTs. On sequencing, they detected V600E mutation in 21 of 23 immunopositive DNTs and in none of the immunonegative DNTs, thus giving a concordance rate of 98% between the two methods. Similarly, Chappe et al. (2013) reported excellent concordance between immunohistochemistry and DNA direct sequencing (k = +0.93). Recently, Rivera et al. (2016) utilized more sensitive methods like whole exome sequencing and

**Table 1**
Clinical details and results of molecular and immunohistochemical assays for DNT patients included in the study.

| Case no. | Age (years)/Sex | Age at seizure onset (years) | Duration of seizures | Tumor location | Extent of resection | Outcome: Engel grade | BRAF mutation | BRAF copy number gain | mTOR pathway markers | | MAPK pathway marker |
|---|---|---|---|---|---|---|---|---|---|---|---|
| | | | | | | | | | p-S6 | p-4EBP1 | p-MAPK |
| 1 | 10/Male | 5 | 5 | Parietal lobe | Complete | 1 | V600E mutation | No gain | Positive (3+) | Positive (2+) | Positive (2+) |
| 2 | 12/Male | 6 | 6 | Temporal lobe | Complete | 1 | Wild-type | Gain | Positive (3+) | Positive (2+) | Positive (3+) |
| 3 | 14/Male | 7 | 7 | Temporal lobe | Complete | 1 | – | – | Positive (3+) | Negative (0) | – |
| 4 | 25/Female | 10 | 15 | Temporal lobe | Complete | 1 | Wild-type | No gain | – | – | – |
| 5 | 10/Male | 6 | 4 | Temporoparietal lobe | Complete | 1 | Wild-type | Gain | Positive (2+) | Negative (0) | Negative (0) |
| 6 | 15/Female | 9 | 6 | Frontal lobe | Complete | 1 | Wild-type | No gain | Positive (3+) | Positive (2+) | Negative (1+) |
| 7 | 14/Male | 6 | 8 | Temporal lobe | Complete | 1 | – | – | Positive (2+) | – | – |
| 8 | 6/Female | 3 | 3 | Temporal lobe | Complete | 1 | Wild-type | Gain | Positive (2+) | Negative (0) | – |
| 9 | 9/Male | 5 | 4 | Temporal lobe | Complete | 1 | Wild-type | No gain | – | – | – |
| 10 | 10/Male | 6 | 4 | Frontal lobe | Complete | 1 | Wild-type | Gain | – | – | – |
| 11 | 14/Female | 7 | 7 | Frontal lobe | Complete | 1 | Wild-type | No gain | – | – | – |
| 12 | 19/Female | 4 | 15 | Frontal lobe | Complete | 1 | Wild-type | No gain | Positive (3+) | Positive (2+) | Negative (0) |
| 13 | 19/Female | 11 | 8 | Temporal lobe | Complete | 1 | Wild-type | No gain | Positive (2+) | Negative (0) | Positive (3+) |
| 14 | 12/Male | 4 | 8 | Temporal lobe | Complete | 1 | Wild-type | No gain | Positive (2+) | Negative (0) | Negative (0) |
| 15 | 11/Male | 4 | 7 | Temporal lobe | Complete | 1 | Wild-type | No gain | Positive (3+) | Negative (0) | – |
| 16 | 12/Male | 6 | 6 | Temporal lobe | Complete | 1 | Wild-type | No gain | Positive (3+) | Negative (0) | Positive (3+) |
| 17 | 28/Male | 20 | 8 | Occipital lobe | Complete | 1 | Wild-type | No gain | Positive (3+) | Positive (2+) | Positive (3+) |
| 18 | 24/Male | 12 | 12 | Parietal lobe | Complete | 1 | Wild-type | No gain | Positive (2+) | Negative (0) | Negative (1+) |
| 19 | 20/Male | 15 | 5 | Temporal lobe | Complete | 1 | Wild-type | Gain | Positive (3+) | – | – |
| 20 | 7/Male | 3 | 4 | Parietal lobe | Complete | 1 | Wild-type | No gain | Positive (2+) | Negative (0) | Positive (2+) |
| 21 | 16/Male | 9 | 7 | Frontal lobe | Complete | 1 | – | – | Positive (2+) | Negative (0) | Negative (0) |
| 22 | 36/Female | 24 | 12 | Temporal lobe | Complete | 1 | Wild-type | No gain | Positive (3+) | Negative (0) | – |
| 23 | 14/Male | 7 | 7 | Temporal lobe | Complete | 1 | – | – | Positive (3+) | Negative (0) | – |
| 24 | 25/Male | 16 | 9 | Parietal lobe | Complete | 1 | Wild-type | No gain | Positive (2+) | Negative (0) | Negative (1+) |
| 25 | 7/Female | 3 | 4 | Occipital lobe | Complete | 1 | Wild-type | No gain | Positive (2+) | Negative (0) | Negative (1+) |
| 26 | 28/Male | 17 | 11 | Temporal lobe, residual | Complete | 1 | – | – | Negative (1+) | Negative (0) | – |
| 27 | 12/Male | 9 | 3 | Frontal lobe | Complete | 1 | Wild-type | No gain | Positive (3+) | Positive (2+) | Positive (3+) |
| 28 | 22/Female | 11 | 11 | Temporal lobe | Complete | 1 | Wild-type | Gain | Negative (0) | Negative (0) | Negative (0) |
| 29 | 17/Male | 13 | 4 | Temporal lobe | Incomplete | 3 | – | – | Negative (0) | Negative (0) | Positive (3+) |
| 30 | 8/Male | 4 | 4 | Temporal lobe, residual | Complete | 1 | Wild-type | Gain | Positive (3+) | – | Positive (3+) |
| 31 | 8/Female | 5 | 3 | Temporal lobe | Complete | 2 | Wild-type | No gain | Positive (3+) | – | – |
| 32 | 9/Male | 4 | 5 | Frontal lobe | Complete | 1 | – | – | Positive (3+) | Negative (0) | Positive (3+) |

Table 1 (*Continued*)

| Case no. | Age (years)/Sex | Age at seizure onset (years) | Duration of seizures | Tumor location | Extent of resection | Outcome: Engel grade | BRAF mutation | BRAF copy number gain | mTOR pathway markers | | MAPK pathway marker |
|---|---|---|---|---|---|---|---|---|---|---|---|
| | | | | | | | | | p-S6 | p-4EBP1 | p-MAPK |
| 33 | 26/Male | 11 | 15 | Temporal lobe | Complete | 1 | Wild-type | Gain | Positive (3+) | – | Negative (1+) |
| 34 | 7/Male | 3 | 4 | Frontal lobe | Complete | 2 | Wild-type | Gain | – | – | – |
| 35 | 18/Male | 6 | 12 | Temporal lobe | Incomplete | 3 | – | – | – | – | – |
| 36 | 15/Male | 9 | 6 | Frontal lobe | Complete | 1 | – | – | – | – | – |
| 37 | 18/Female | 12 | 6 | Temporal lobe | Complete | 1 | – | – | – | – | – |
| 38 | 22/Male | 4 | 18 | Temporal lobe | Complete | 1 | – | – | – | – | – |
| 39 | 14/Male | 7 | 7 | Frontal lobe | Complete | 1 | – | – | – | – | – |
| 40 | 26/Male | 4 | 22 | Temporal lobe | Complete | 1 | – | – | – | – | – |
| 41 | 18/Male | 13 | 5 | Frontal lobe | Complete | 1 | – | – | – | – | – |
| 42 | 4/Male | 3 | 1 | Temporal lobe | Complete | 1 | – | – | – | – | – |
| 43 | 12/Male | 5 | 7 | Parietal lobe | Complete | 2 | – | – | – | – | – |
| 44 | 14/Male | 4 | 10 | Occipital lobe | Incomplete | 2 | – | – | – | – | – |
| 45 | 12/Female | 7 | 5 | Temporal lobe | Complete | 1 | – | – | – | – | – |
| 46 | 28/Female | 20 | 8 | Temporal lobe | Complete | 1 | – | – | – | – | – |
| 47 | 12/Male | 6 | 6 | Temporal lobe | Complete | 1 | – | – | – | – | – |
| 48 | 37/Female | 16 | 21 | Frontal lobe | Complete | 1 | – | – | – | – | – |
| 49 | 16/Male | 8 | 8 | Temporal lobe | Complete | 2 | – | – | – | – | – |
| 50 | 10/Male | 6 | 4 | Temporal lobe | Complete | 1 | – | – | – | – | – |
| 51 | 16/Male | 8 | 8 | Temporal lobe | Complete | 1 | – | – | – | – | – |
| 52 | 16/Male | 9 | 7 | Parietal lobe | Complete | 1 | – | – | – | – | – |
| 53 | 6/Male | 3 | 3 | Parietal lobe | Incomplete | 2 | – | – | – | – | – |
| 54 | 14/Male | 7 | 7 | Occipital lobe | Complete | 2 | – | – | – | – | – |
| 55 | 14/Male | 7 | 7 | Frontal lobe | Complete | 1 | – | – | – | – | – |
| 56 | 5/Male | 3 | 2 | Temporal lobe | Complete | 1 | – | – | – | – | – |
| 57 | 17/Male | 8 | 9 | Parietal lobe | Complete | 1 | – | – | – | – | – |
| 58 | 20/Male | 12 | 8 | Posterior fossa | Complete | 1 | – | – | – | – | – |
| 59 | 16/Male | 13 | 3 | Temporal lobe | Complete | 1 | – | – | – | – | – |
| 60 | 19/Male | 8 | 11 | Temporal lobe | Complete | 1 | – | – | – | – | – |
| 61 | 2/Female | 1 | 1 | Frontal lobe | Complete | 1 | – | – | – | – | – |
| 62 | 9/Female | 4 | 5 | Parietal lobe | Complete | 1 | – | – | – | – | – |
| 63 | 6/Male | 3 | 3 | Temporal lobe | Complete | 1 | – | – | – | – | – |
| 64 | 29/Male | 12 | 17 | Temporal lobe | Complete | 1 | – | – | – | – | – |

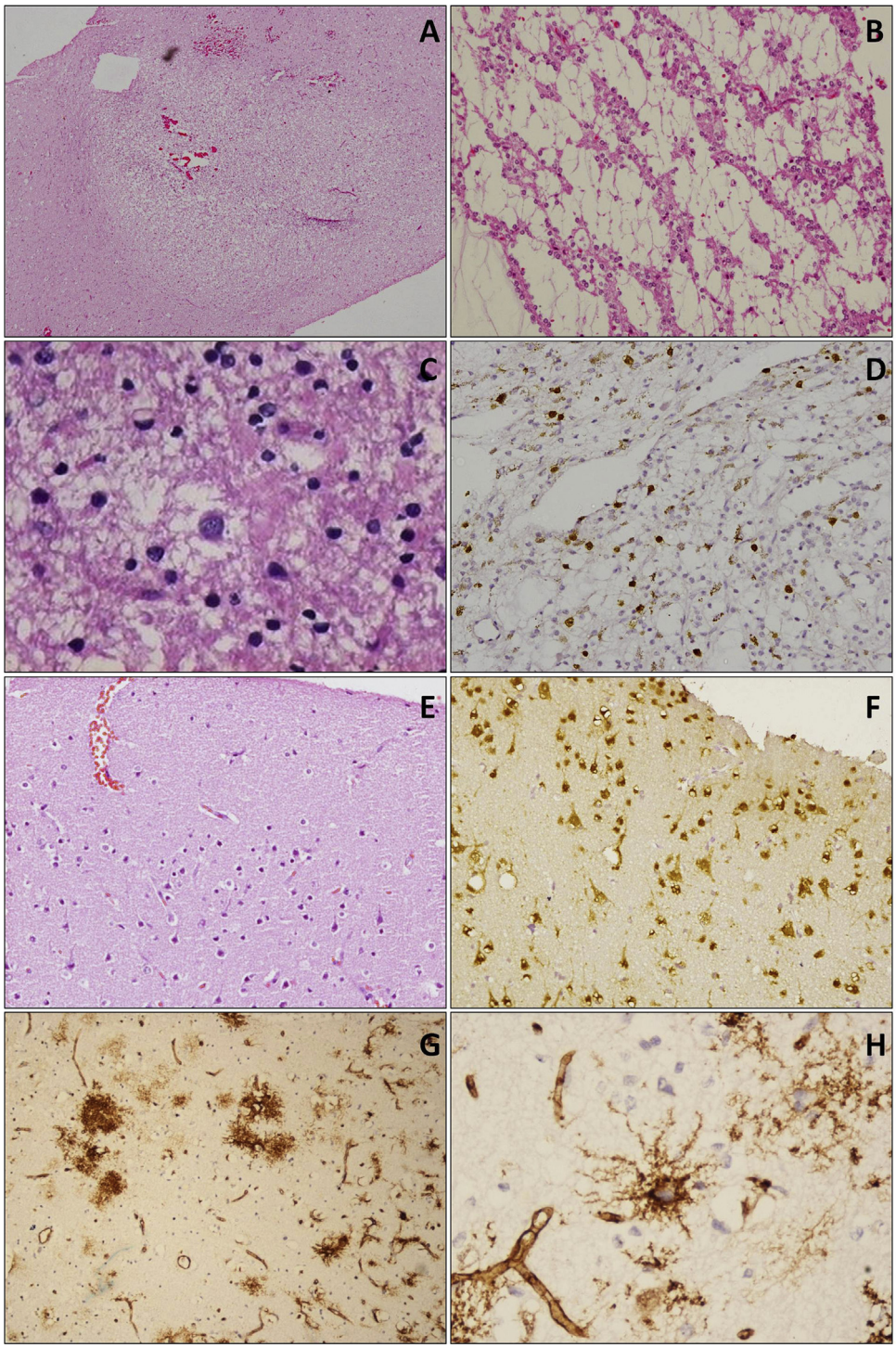


**Fig. 1.** Histomorphology of DNT: Tumor nodule (A; HE, 100x) composed of perpendicular arrays of oligodendroglial-like cells in a myxoid background (B; HE, 200x) with interspersed floating neurons (C; HE, 400x) highlighted by NeuN staining (D; IHC, 200x). Cortex adjacent to the tumor shows cortical dysplasia with loss of laminar architecture (E; HE, 100x) highlighted by NeuN staining (F; IHC, 200x); dysplastic neurons show bush-like positivity for CD34 (G; IHC, 200 x and H; IHC, 400x).

next-generation sequencing to identify *BRAF* V600E mutation in a large series of DNTs; none of the cases analyzed by them harboured V600E mutation. We also performed sequencing and demonstrated *BRAF* V600E mutation at a low frequency (in 3.7% of cases), similar to its absence in the study by Rivera et al. (2016). Thus, there is a marked variability in the frequency of *BRAF* V600E mutation in DNTs in different studies, which may be attributed to different methodologies used in each of them (Table 2). While Sanger sequencing has been considered the gold standard for detecting mutations in DNA, it also has certain limitations. It requires an allele frequency of about 15–20% as the DNA mutation detection threshold. Factors like tumor heterogeneity and contamination with normal cells may affect the rate of mutation detection. Although tissue sections with more than 80% of tumor cells were used for DNA extraction and *BRAF* V600E detection, it is possible that we may have missed this mutation in a few cases, owing to tumor heterogeneity. Newer methods with higher threshold for detection of mutations, such as deep next-generation sequencing may

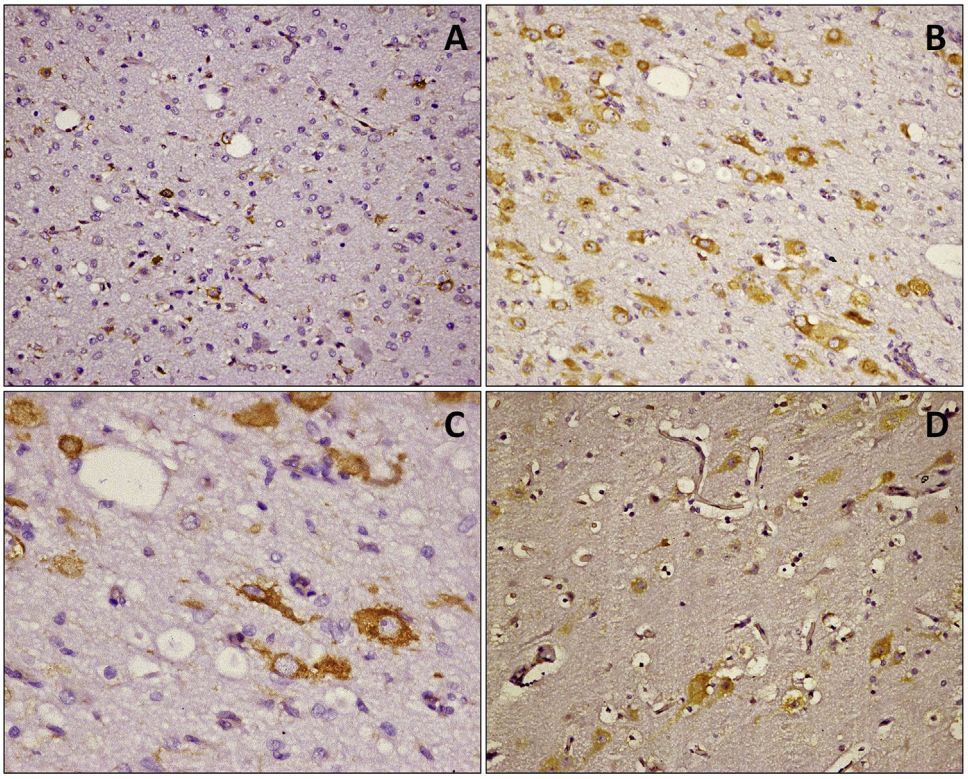


**Fig. 2.** Immunostaining for mTOR pathway marker p-S6: Cases of DNT showing 2+ immunopositivity (A; IHC, 200x) and 3+ immunopositivity (B; IHC, 200x) for p-S6; high magnification shows immunopositivity in floating neurons (C; IHC, 400x); neurons in the adjacent dysplstic cortex showing p-S6 immunopositivity (D; IHC, 200x).

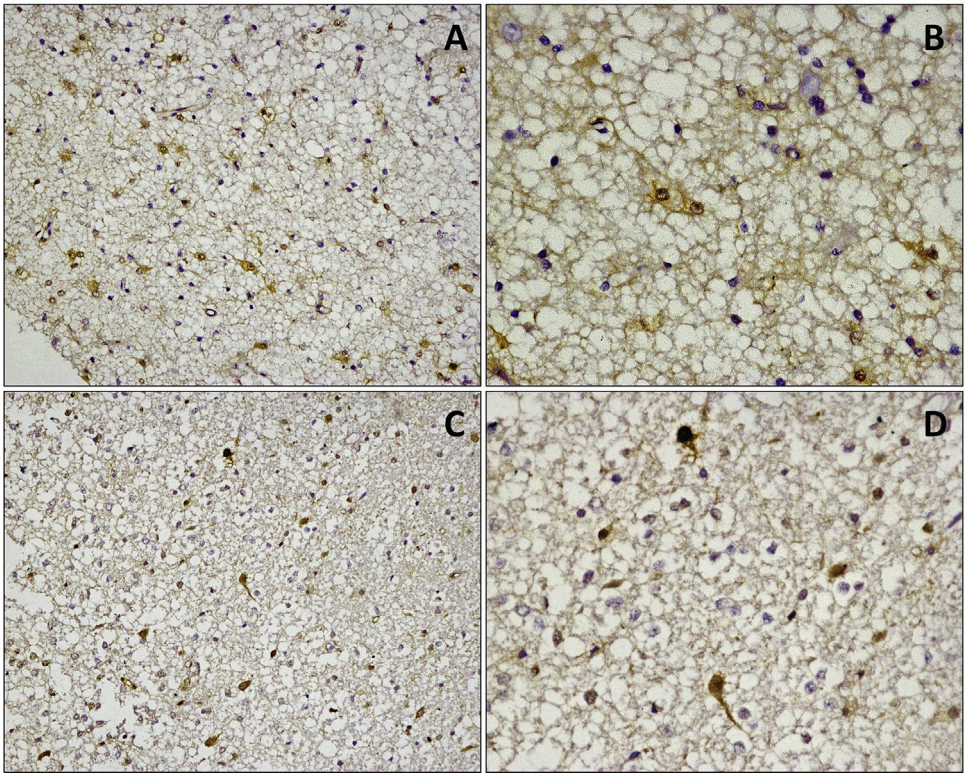


**Fig. 3.** Immunostaining for mTOR and MAPK pathway markers: Cases of DNT showing 2+ immunopositivity for p-4EBP1 (A, IHC, 200x; B, IHC, 400x) and 3+ immunopositivity for p-MAPK (C, IHC, 200x; D, IHC, 400x).

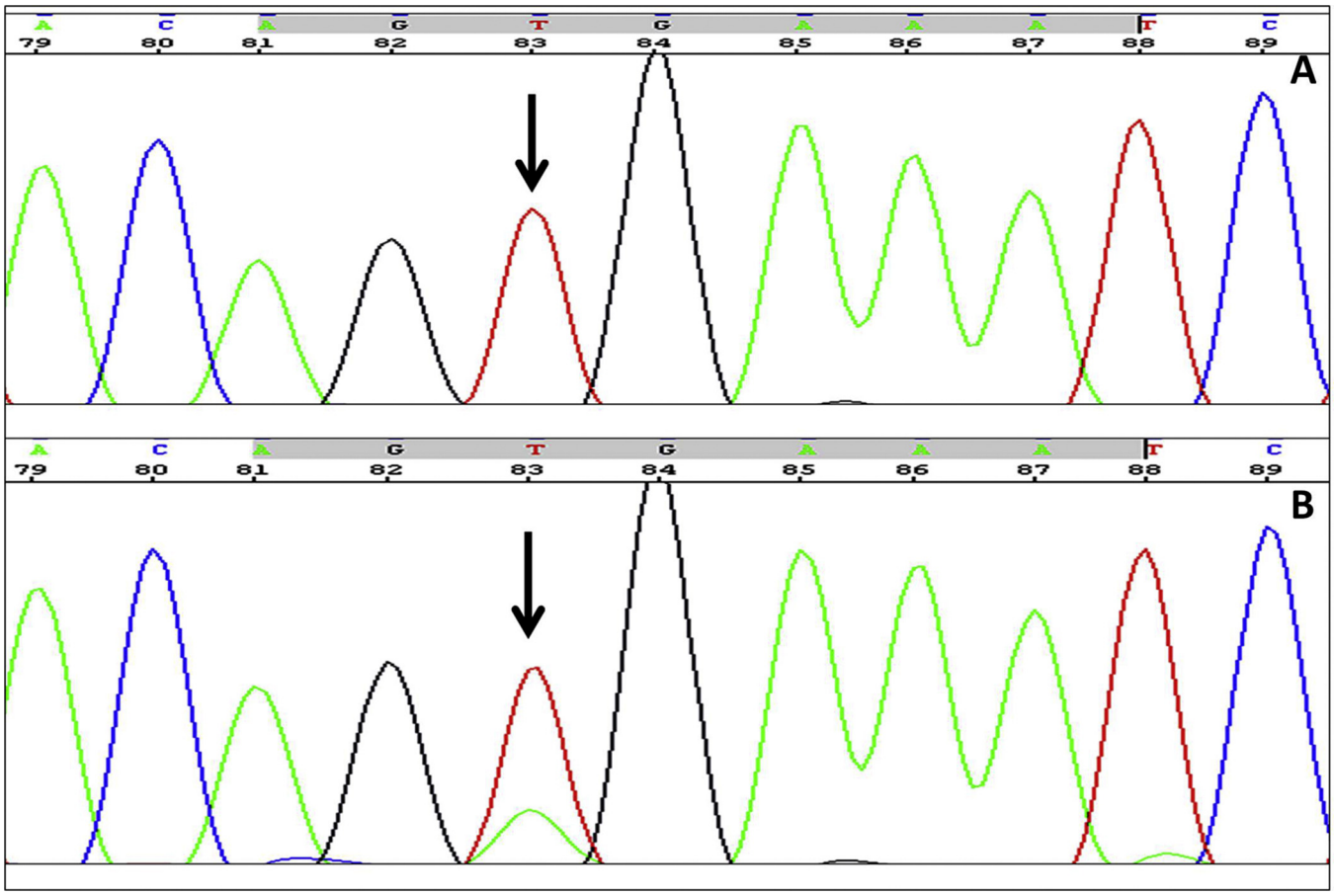


**Fig. 4.** Electropherogram showing wild-type *BRAF* (A) and *BRAF* V600E mutation (B).

**Table 2**
Methodology used and frequency of BRAF V600E mutation in previous studies on Dysembryoplastic neuroepithelial tumors.

| Reference | Number of cases | Methodology used | Frequency of BRAF V600E mutation |
|---|---|---|---|
| Dougherty et al., 2010 | 3 | Sanger sequencing | 0% |
| Schindler et al., 2011 | 4 | Sequencing | 0% |
| Horbinski et al., 2012 | 1 | RT-PCR and post-PCR fluorescence melting curve analysis | 0% |
| Chappe et al., 2013 | 11 | HRM, sequencing and immunohistochemistry | 30% |
| Zhang et al., 2013 | 2 | Next-generation sequencing | 0% |
| Lee et al., 2015 | 51 | Sanger sequencing | 51% |
| Prabowo et al., 2014 | 77 | Sanger sequencing and immunohistochemistry | 30% |
| Gierke et al., 2016 | 11 | Restriction-based polymerase chain reaction and immunohistochemistry | 9% |
| Rivera et al., 2016 | 43 | Next-generation sequencing, Fluidigm access array system | 0% |
| Present study, 2016 | 27 | Sanger sequencing | 3.7% |

have given a better estimation of BRAF V600E mutation and this remains the limitation of our study. The low frequency of BRAF mutation in our study may also be attributed to differences in ethnicity, as also speculated by Prabowo et al. (2014) and Lee et al. (2015) as an explanation for the high frequency of BRAF mutation in their studies when compared to other reports on DNTs. Identification of this mutation in a small number of DNTs indicates a shared pathogenetic mechanism of a subset of these tumors with GG and PXA, both of which are also associated with intractable epilepsy and show this mutation as well.

Copy number alterations have not been extensively analyzed in DNTs. Roth et al., in 2015, reported a possible case of DNT which on single nucleotide polymorphism (SNP)-based array analysis showed deletion of 7q34, resulting in fusion of *BRAF* with the *FAM131B* gene. Gessi et al. evaluated 7 supratentorial midline DNTs and found gain of 8p12; however, no copy number change was present at 7q34. In our study, we identified gain of the *BRAF* locus in 33.3% cases. Ours is the first study to demonstrate *BRAF* gain in DNTs, emphasizing that *BRAF* V600E mutation and *BRAF* fusion are not the only *BRAF* alterations that may be seen in these tumors. This finding is in concordance with previous reports of gain of chromosome 7q in DNTs available in literature; however, its role in DNT pathogenesis needs further elucidation (Prabowo et al., 2015). Absence of V600E mutation should therefore prompt an analysis of *BRAF* copy number, as there lies the possibility that patients harbouring *BRAF* gain may stand to benefit from *BRAF* inhibitors.

The mTOR pathway is a key intracellular signalling pathway that responds to stimulation by various growth factors and nutrients, and whose role in tumor cell growth and proliferation is well established. Activation of mTOR by phosphorylation causes activation of its downstream substrate 4EBP1, which in turn releases the eukaryotic initiation factor 4E (eIF4E). eIF4E interacts with p-eukaryotic

initiation factor 4G (eIF4G) to activate cap-dependent mRNA translation which enhances cell size and cell proliferation (Holmes et al., 2007). mTOR also increases cell size and proliferation by phosphorylating downstream p70S6K, leading to activation of S6 protein. Previous studies have demonstrated activation of the mTOR signalling pathway in lesions associated with intractable epilepsy, such as FCD, and in some brain tumors (Baybis et al., 2004; Hütt-Cabezas et al., 2013; Ljungberg et al., 2006; Mueller et al., 2012; Schick et al., 2007). However, there are very few studies on the same in DNTs. Till date, only two studies have assessed the mTOR pathway in DNTs. Boer et al. (2010) evaluated nine cases of DNT for activation of mTOR signalling using 8 antibodies, including p-S6 and p-4EBP1. In their study, p-S6 immunopositivity was noted in few neuronal cells, with a LI of $5 \pm 3\%$, while p-4EBP1 immunopositivity was similar to that in control samples (LI = $1 \pm 0.2\%$). Based on the low labelling indices for these markers, the authors concluded that mTOR pathway activation is not detected in DNTs. Interestingly, normal appearing peritumoral cortex from 3 GGs and 2 DNTs also showed immunopositivity for p-S6 (LI = $6 \pm 3\%$) and p-4EBP1 (LI = $1 \pm 0.2\%$), which was higher than that for control tissues (p-S6 LI = $3 \pm 1\%$ and p-4EBP1 LI = $1 \pm 0.5\%$). However, the authors did not comment on this finding. A subsequent study by Prabowo et al. (2014) identified p-S6 immunoreactivity as a marker for mTOR pathway activation in the neuronal cells in 31 of 77 (40%) DNTs analyzed, which was seen in association with *BRAF* V600E mutation. In our study, we identified immunopositivity for p-S6, the activated form of S6 protein, as well as for 4EBP1, indicating mTOR pathway activation in 89.7% of DNTs. This immunoreactivity was noted predominantly in the neuronal cell component, indicating that it is this cellular component of the tumor that may be responsible for its epileptogenic potiential. We also noted that p-S6 immunopositivity was present in dysmorphic neurons in the dysplastic cortex adjacent to the tumor. This is in concordance with findings of previous studies that have reported activation of mTOR pathway in FCD and other malformations of cortical development (Nguyen et al., 2015). Thus, it appears that enhanced mTOR signalling is central to the pathogenesis of intractable epilepsy-associated lesions, whether tumoral or non-tumoral. Although a few studies on pediatric low grade gliomas have reported a worse outcome in patients whose tumors demonstrated mTOR activation (Mueller et al., 2012), no significant association was noted between seizure-free outcome and enhanced mTOR signalling in our series.

Prabowo et al. (2014) are also the first group to demonstrate the association of mTOR pathway activation with *BRAF* V600E mutation in DNTs. This association has previously been demonstrated in other tumors such as papillary carcinoma thyroid and malignant melanoma (Galanopoulou et al., 2012; Populo et al., 2010). In our study, all except one case with *BRAF* alterations showed association with enhanced mTOR pathway signalling. While cases with copy number gain showed p-S6 immunoreactivity with or without p-4EBP1 positivity, the case with V600E mutation showed immnopositivity with both p-S6 and p-4EBP1. This suggests that different *BRAF* alterations affect the various components of the mTOR pathway differently. These findings will help to further elucidate the molecular pathogenesis of DNTs.

The MAPK pathway links extracellular signals to cellular processes such as cell growth, proliferation, differentiation, and migration, and dysregulation of this pathway plays an important role in cancer development and progression (Dhillon et al., 2007). With respect to brain tumors, this pathway has been shown to be activated in pilocytic astrocytomas, as well as in high grade gliomas (Cin et al., 2011; Forshew et al., 2009; Jones et al., 2012). In DNTs, this pathway has not been evaluated till date. We performed IHC for p-MAPK and demonstrated positivity in 50% of cases, which was irrespective of presence of *BRAF* alterations. This suggests that while MAPK activation plays a role in DNT pathogenesis, it may be independent of *BRAF*, and may involve activation of other upstream molecules, or some epigenetic modifications.

## 5. Conclusions

Ours is the first study to demonstrate *BRAF* copy number gain in DNTs, highlighting that *BRAF* alterations other than V600E mutation can lead to activation of downstream pathways. We demonstrate activation of the mTOR pathway in DNTs, as in other epilepsy associated lesions, as evidenced by increased immunoreactivity for mTOR pathway components p-S6 and p-4EBP1, thus providing a link in the pathogenesis of these lesions. The identification of p-S6 positivity in dysplastic cortex adjacent to DNTs further consolidates the hypothesis that enhanced mTOR signalling is central to the pathogenesis of epilepsy associated lesions, whether tumoral or non-tumoral. These findings suggest that rapamycin analogs that act as inhibitors of mTOR pathway could serve as a therapeutic option for DNT patients presenting with intractable epilepsy, and that markers of mTOR pathway activation could serve as clinically relevant biomarkers for identification of patients that may benefit from mTOR inhibitors, thus optimizing their therapeutic potential. MAPK activation, when identified, can also similarly serve as a therapeutic target. Thus, our results will ultimately pave the way for development of targeted therapies involving specific downstream targets in these pathogenetic pathways in the future, which may be most relevant for patients whose tumors are incompletely resected, and those with residual seizures after surgery.

## Disclosure

None of the authors has any conflict of interest to disclose.

## Funding

This work was supported financially by the J C Bose Fellowship awarded to the corresponding author Dr Chitra Sarkar, as well as the grants to the Centre of Excellence for Epilepsy, a collaborative project between National Brain Research Centre, Manesar, and All India Institute of Medical Sciences, New Delhi (grant no.: BT/01/COE/09/08 and BT/Bio-Care/07/9816/2013-2014 funded by Department of Biotechnology, Ministry of Science and Technology, Govt. of India). These funding sources did not play a role in the study design, collection, analysis or interpretation of data, writing of the report, or in the decision to submit the article for publication.

## Acknowledgements

The authors would like to thank Dr Mohammed Faruq from Institute of Genomics and Integrative Biology – Council of Scientific and Industrial Research for assistance with BRAF sequencing, and all technical staff from the Neuropathology lab, AIIMS, for their assistance with immunohistochemistry.

## References

Baybis, M., Yu, J., Lee, A., Golden, J.A., Weiner, H., McKhann 2nd, G., Aronica, E., Crino, P.B., 2004. mTOR cascade activation distinguishes tubers from focal cortical dysplasia. Ann. Neurol. 56, 478–487.

Berghoff, A.S., Preusser, M., 2014. *BRAF* alterations in brain tumours: molecular pathology and therapeutic opportunities. Curr. Opin. Neurol. 27, 689–696.

Biernat, W., Huang, H., Yokoo, H., Kleihues, P., Ohgaki, H., 2004. Predominant expression of mutant EGFR (EGFRvIII) is rare in primary glioblastomas. Brain Pathol. 14, 131–136.

Blümcke, I., Thom, M., Aronica, E., Armstrong, D.D., Vinters, H.V., Palmini, A., Jacques, T.S., Avanzini, G., Barkovich, A.J., Battaglia, G., Becker, A., Cepeda, C., Cendes, F., Colombo, N., Crino, P., Cross, J.H., Delalande, O., Dubeau, F., Duncan, J., Guerrini, R., Kahane, P., Mathern, G., Najm, I., Ozkara, C., Raybaud, C., Represa, A., Roper, S.N., Salamon, N., Schulze-Bonhage, A., Tassi, L., Vezzani, A., Spreafico, R., 2011. The clinicopathologic spectrum of focal cortical dysplasias:

a consensus classification proposed by an ad hoc task force of the ILAE diagnostic methods commission. Epilepsia 52, 158–174.
Boer, K., Troost, D., Timmerman, W., Spliet, W.G.M., van Rijen, P.C., Aronica, E., 2010. Pi3K-mTOR signaling and AMOG expression in epilepsy-associated glioneuronal tumors. Brain Pathol. 20, 234–244.
Chan, C.H., Bittar, R.G., Davis, G.A., Kalnins, R.M., Fabinyi, G.C., 2006. Long-term seizure outcome following surgery for dysembryoplastic neuroepithelial tumor. J. Neurosurg. 104, 62–69.
Chapman, P.B., Hauschild, A., Robert, C., Haanen, J.B., Ascierto, P., Larkin, J., Dummer, R., Garbe, C., Testori, A., Maio, M., Hogg, D., Lorigan, P., Lebbe, C., Jouary, T., Schadendorf, D., Ribas, A., O'Day, S.J., Sosman, J.A., Kirkwood, J.M., Eggermont, A.M., Dreno, B., Nolop, K., Li, J., Nelson, B., Hou, J., Lee, R.J., Flaherty, K.T., McArthur, G.A., BRIM-3 Study Group, 2011. Improved survival with vemurafenib in melanoma with BRAF V600E mutation. New Engl. J. Med. 364, 2507–2516.
Chappe, C., Padovani, L., Scavarda, D., Forest, F., Nanni-Metellus, I., Loundou, A., Mercurio, S., Fina, F., Lena, G., Colin, C., Figarella-Branger, D., 2013. Dysembryoplastic neuroepithelial tumors share with pleomorphic xanthoastrocytomas and gangliogliomas *BRAF* mutation and expression. Brain Pathol. 23, 574–583.
Cin, H., Meyer, C., Herr, R., Janzarik, W.G., Lambert, S., Jones, D.T., Jacob, K., Benner, A., Witt, H., Remke, M., Bender, S., Falkenstein, F., Van Anh, T.N., Olbrich, H., von Deimling, A., Pekrun, A., Kulozik, A.E., Gnekow, A., Scheurlen, W., Witt, O., Omran, H., Jabado, N., Collins, V.P., Brummer, T., Marschalek, R., Lichter, P., Korshunov, A., Pfister, S.M., 2011. Oncogenic FAM131B-*BRAF* fusion resulting from 7q34 deletion comprises an alternative mechanism of MAPK pathway activation in pilocytic astrocytoma. Acta Neuropathol. 121, 763–774.
Collins, V.P., Jones, D.T., Giannini, C., 2015. Pilocytic astrocytoma: pathology, molecular mechanisms and markers. Acta Neuropathol. 129, 775–788.
Daumas-Duport, C., Scheithauer, B.W., Chodkiewicz, J.P., Laws, E.R., Vedrenne, C., 1988. Dysembryoplastic neuroepithelial tumor: a surgically curable tumor of young patients with intractable partial seizures: report of thirty-nine cases. Neurosurgery 23, 545–556.
Dhillon, A.S., Hagan, S., Rath, O., Kolch, W., 2007. MAP kinase signalling pathways in cancer. Oncogene 26, 3279–3290.
Dougherty, M.J., Santi, M., Brose, M.S., Ma, C., Resnick, A.C., Sievert, A.J., Storm, P.B., Biegel, J.A., 2010. Activating mutations in *BRAF* characterize a spectrum of pediatric low-grade gliomas. Neuro Oncol. 12, 621–630.
Engel Jr., J., 1993. Surgical Treatment of the Epilepsies. Raven Press, New York.
Faustino, A., Couto, J.P., Pópulo, H., Rocha, A.S., Pardal, F., Cameselle-Teijeiro, J.M., Lopes, J.M., Sobrinho-Simões, M., Soares, P., 2012. mTOR pathway overactivation in *BRAF* mutated papillary thyroid carcinoma. J. Clin. Endocrinol. Metab. 97, E1139–1149.
Flaherty, K.T., Robert, C., Hersey, P., Nathan, P., Garbe, C., Milhem, M., Demidov, L.V., Hassel, J.C., Rutkowski, P., Mohr, P., Dummer, R., Trefzer, U., Larkin, J.M., Utikal, J., Dreno, B., Nyakas, M., Middleton, M.R., Becker, J.C., Casey, M., Sherman, L.J., Wu, F.S., Ouellet, D., Martin, A.M., Patel, K., Schadendorf, D., METRIC Study Group, 2012. Improved survival with MEK inhibition in BRAF-mutated melanoma. New Engl. J. Med. 367, 107–114.
Forshew, T., Tatevossian, R.G., Lawson, A.R., Ma, J., Neale, G., Ogunkolade, B.W., Jones, T.A., Aarum, J., Dalton, J., Bailey, S., Chaplin, T., Carter, R.L., Gajjar, A., Broniscer, A., Young, B.D., Ellison, D.W., Sheer, D., 2009. Activation of the ERK/MAPK pathway: a signature genetic defect in posterior fossa pilocytic astrocytomas. J. Pathol. 218, 172–181.
Galanopoulou, A.S., Gorter, J.A., Cepeda, C., 2012. Finding a better drug for epilepsy: the mTOR pathway as an antiepileptogenic target. Epilepsia 53, 1119–1130.
Gessi, M., Hattingen, E., Dörner, E., Goschzik, T., Dreschmann, V., Waha, A., Pietsch, T., 2016. Dysembryoplastic neuroepithelial tumor of the septum pellucidum and the supratentorial midline: histopathologic, neuroradiologic, and molecular features of 7 cases. Am. J. Surg. Pathol. 40 (June (6)), 806–811.
Gierke, M., Sperveslage, J., Schwab, D., Beschorner, R., Ebinger, M., Schuhmann, M.U., Schittenhelm, J., 2016. Analysis of IDH1-R132 mutation, *BRAF* V600 mutation and KIAA1549-*BRAF* fusion transcript status in central nervous system tumors supports pediatric tumor classification. J. Cancer Res. Clin. Oncol. 142, 89–100.
Hütt-Cabezas, M., Karajannis, M.A., Zagzag, D., Shah, S., Horkayne-Szakaly, I., Rushing, E.J., Cameron, J.D., Jain, D., Eberhart, C.G., Raabe, E.H., Rodriguez, F.J., 2013. Activation of mTORC1/mTORC2 signaling in pediatric low-grade glioma and pilocytic astrocytoma reveals mTOR as a therapeutic target. Neuro Oncol. 15, 1604–1614.
Holmes, G.L., Stafstrom, C.E., Tuberous Sclerosis Study Group, 2007. Tuberous sclerosis complex and epilepsy: recent developments and future challenges. Epilepsia 48, 617–630.
Horbinski, C., Nikiforova, M.N., Hagenkord, J.M., Hamilton, R.L., Pollack, I.F., 2012. Interplay among *BRAF*, p16, p53, and MIB1 in pediatric low-grade gliomas. Neuro Oncol. 14, 777–789.
Jones, D.T., Gronych, J., Lichter, P., Witt, O., Pfister, S.M., 2012. MAPK pathway activation in pilocytic astrocytoma. Cell. Mol. Life. Sci. 69, 1799–1811.
Kakkar, A., Biswas, A., Goyal, N., Suri, V., Sharma, M.C., Gupta, D., Julka, P.K., Sarkar, C., 2015. The expression of cyclin D1, VEGF, EZH2 and H3K27me3 in atypical teratoid/rhabdoid tumors of CNS: possible role in targeted therapy. Appl. Immunohistochem. Mol. Morphol. (October (13)) (Epub ahead of print).
Kirkpatrick, P.J., Honavar, M., Janota, I., Polkey, C.E., 1993. Control of temporal lobe epilepsy following en bloc resection of low-grade tumors. J. Neurosurg. 78, 19–25.
Kumar, A., Pathak, P., Purkait, S., Faruq, M., Jha, P., Mallick, S., Suri, V., Sharma, M.C., Suri, A., Sarkar, C., 2015. Oncogenic KIAA1549-BRAF fusion with activation of the MAPK/ERK pathway in pediatric oligodendrogliomas. Cancer Genet. 208, 91–95.
Lee, D.Y., Chung, C.K., Hwang, Y.S., Choe, G., Chi, J.G., Kim, H.J., Cho, B.K., 2000. Dysembryoplastic neuroepithelial tumor: radiological findings (including PET, SPECT, and MRS) and surgical strategy. J. Neurooncol. 47, 167–174.
Lee, J., Lee, B.L., Joo, E.Y., Seo, D.W., Hong, S.B., Hong, S.C., Suh, Y.L., Lee, M., 2009. Dysembryoplastic neuroepithelial tumors in pediatric patients. Brain Dev. 31, 671–681.
Lee, D., Cho, Y.H., Kang, S.Y., Yoon, N., Sung, C.O., Suh, Y.L., 2015. *BRAF* V600E mutations are frequent in dysembryoplastic neuroepithelial tumors and subependymal giant cell astrocytomas. J. Surg. Oncol. 111, 359–364.
Ljungberg, M.C., Bhattacharjee, M.B., Lu, Y., Armstrong, D.L., Yoshor, D., Swann, J.W., Sheldon, M., D'Arcangelo, G., 2006. Activation of mammalian target of rapamycin in cytomegalic neurons of human cortical dysplasia. Ann. Neurol. 60, 420–429.
Mueller, S., Phillips, J., Onar-Thomas, A., Romero, E., Zheng, S., Wiencke, J.K., McBride, S.M., Cowdrey, C., Prados, M.D., Weiss, W.A., Berger, M.S., Gupta, N., Haas-Kogan, D.A., 2012. PTEN promoter methylation and activation of the PI3K/Akt/mTOR pathway in pediatric gliomas and influence on clinical outcome. Neuro Oncol. 14, 1146–1152.
Nguyen, L.H., Brewster, A.L., Clark, M.E., Regnier-Golanov, A., Sunnen, C.N., Patil, V.V., D'Arcangelo, G., Anderson, A.E., 2015. mTOR inhibition suppresses established epilepsy in a mouse model of cortical dysplasia. Epilepsia 56, 636–646.
Nigro, J.M., Takahashi, M.A., Ginzinger, D.G., Law, M., Passe, S., Jenkins, R.B., Aldape, K., 2001. Detection of 1p and 19q loss in oligodendroglioma by quantitative microsatellite analysis: a real-time quantitative polymerase chain reaction assay. Am. J. Pathol. 158, 1253–1262.
Populo, H., Soares, P., Rocha, A.S., Silva, P., Lopes, J.M., 2010. Evaluation of the mTOR pathway in ocular (uvea and conjunctiva) melanoma. Melanoma Res. 20, 107–117.
Prabowo, A.S., Iyer, A.M., Veersema, T.J., Anink, J.J., Schouten-van Meeteren, A.Y., Spliet, W.G., van Rijen, P.C., Ferrier, C.H., Capper, D., Thom, M., Aronica, E., 2014. *BRAF* V600E mutation is associated with mTOR signaling activation in glioneuronal tumors. Brain Pathol. 24, 52–66.
Prabowo, A.S., van Thuijl, H.F., Scheinin, I., Sie, D., van Essen, H.F., Iyer, A.M., Spliet, W.G., Ferrier, C.H., van Rijen, P.C., Veersema, T.J., Thom, M., Schouten-van Meeteren, A.Y., Reijneveld, J.C., Ylstra, B., Wesseling, P., Aronica, E., 2015. Landscape of chromosomal copy number aberrations in gangliogliomas and dysembryoplastic neuroepithelial tumours. Neuropathol. Appl. Neurobiol. 41, 743–755.
Ren, G., Liu, X., Mao, X., Zhang, Y., Stankiewicz, E., Hylands, L., Song, R., Berney, D.M., Clark, J., Cooper, C., Lu, Y.J., 2012. Identification of frequent *BRAF* copy number gain and alterations of RAF genes in Chinese prostate cancer. Genes. Chromosomes Cancer 51, 1014–10123.
Rivera, B., Gayden, T., Carrot-Zhang, J., Naadaf, J., Boshari, T., Faury, D., Zeinieh, M., Blanc, R., Burk, D.L., Fahiminiya, S., Bareke, E., Schüller, U., Monoranu, C.M., Sträter, R., Kerl, K., Niederstadt, T., Kurlemann, G., Ellezam, B., Michalak, Z., Thom, M., Lockhart, P.J., Leventer, R.J., Ohm, M., MacGregor, D., Jones, D., Karamchandani, J., Greenwood, C.M., Berghuis, A.M., Bens, S., Siebert, R., Zakrzewska, M., Liberski, P.P., Zakrzewski, K., Sisodiya, S.M., Paulus, W., Albrecht, S., Hasselblatt, M., Jabado, N., Foulkes, W.D., Majewski, J., 2016. Germline and somatic FGFR1 adnormalities in dysembryoplastic neuroepithelial tumors. Acta Neuropathol. 131, 847–863.
Roth, J.J., Santi, M., Pollock, A.N., Harding, B.N., Rorke-Adams, L.B., Tooke, L.S., Biegel, J.A., 2015. Chromosome band 7q34 deletions resulting in KIAA1549-BRAF and FAM131B-BRAF fusions in pediatric low-grade gliomas. Brain Pathol. 25, 182–192.
Sakuta, R., Otsubo, H., Nolan, M.A., Weiss, S.K., Hawkins, C., Rutka, J.T., Chuang, N.A., Chuang, S.H., Snead 3rd, O.C., 2005. Recurrent intractable seizures in children with cortical dysplasia adjacent to dysembryoplastic neuroepithelial tumor. J. Child Neurol. 20, 377–384.
Sandberg, D.I., Ragheb, J., Dunoyer, C., Bhatia, S., Olavarria, G., Morrison, G., 2005. Surgical outcomes and seizure control rates after resection of dysembryoplastic neuroepithelial tumors. Neurosurg. Focus. 18, E5.
Sarkar, C., Sharma, M.C., Deb, P., Singh, V.P., Chandra, P.S., Gupta, A., Tripathi, M., Bhatia, M., Gaikwad, S., Bal, C.S., Jain, S., 2006. Neuropathological spectrum of lesions associated with intractable epilepsies: a 10-year experience with a series of 153 resections. Neurol. India 54, 144–150.
Sasaki, H., Maekawa, M., Tatematsu, T., Okuda, K., Moriyama, S., Yano, M., Fujii, Y., 2015. Increased *BRAF* copy number in lung adenocarcinoma. Oncol. Lett. 9, 709–712.
Schick, V., Majores, M., Engels, G., Hartmann, W., Elger, C.E., Schramm, J., Schoch, S., Becker, A.J., 2007. Differential Pi3K-pathway activation in cortical tubers and focal cortical dysplasias with balloon cells. Brain Pathol. 17, 165–173.
Schindler, G., Capper, D., Meyer, J., Janzarik, W., Omran, H., Herold-Mende, C., Schmieder, K., Wesseling, P., Mawrin, C., Hasselblatt, M., Louis, D.N., Korshunov, A., Pfister, S., Hartmann, C., Paulus, W., Reifenberger, G., von Deimling, A., 2011. Analysis of *BRAF* V600E mutation in 1,320 nervous system tumors reveals high mutation frequencies in pleomorphic xanthoastrocytoma, ganglioglioma and extra-cerebellar pilocytic astrocytoma. Acta Neuropathol. 121, 397–405.
Sharma, M.C., Jain, D., Gupta, A., Sarkar, C., Suri, V., Garg, A., Gaikwad, S.B., Chandra, P.S., 2009. Dysembryoplastic neuroepithelial tumor: a clinicopathological study of 32 cases. Neurosurg. Rev. 32, 161–169.

Takahashi, A., Hong, S.C., Seo, D.W., Hong, S.B., Lee, M., Suh, Y.L., 2005. Frequent association of cortical dysplasia in dysembryoplastic neuroepithelial tumor treated by epilepsy surgery. Surg. Neurol. 64, 419–427.

Zhang, J., Wu, G., Miller, C.P., Tatevossian, R.G., Dalton, J.D., Tang, B., Orisme, W., Punchihewa, C., Parker, M., Qaddoumi, I., Boop, F.A., Lu, C., Kandoth, C., Ding, L., Lee, R., Huether, R., Chen, X., Hedlund, E., Nagahawatte, P., Rusch, M., Boggs, K., Cheng, J., Becksfort, J., Ma, J., Song, G., Li, Y., Wei, L., Wang, J., Shurtleff, S., Easton, J., Zhao, D., Fulton, R.S., Fulton, L.L., Dooling, D.J., Vadodaria, B., Mulder, H.L., Tang, C., Ochoa, K., Mullighan, C.G., Gajjar, A., Kriwacki, R., Sheer, D., Gilbertson, R.J., Mardis, E.R., Wilson, R.K., Downing, J.R., Baker, S.J., Ellison, D.W., St. Jude Children's Research Hospital–Washington University Pediatric Cancer Genome Project, 2013. Whole-genome sequencing identifies genetic alterations in pediatric low-grade gliomas. Nat. Genet. 45, 602–612.